SAND2021-4950PE

DECOVALEX2023 WORKSHOP

DECOVALEX 2023 TASK B: MAGIC

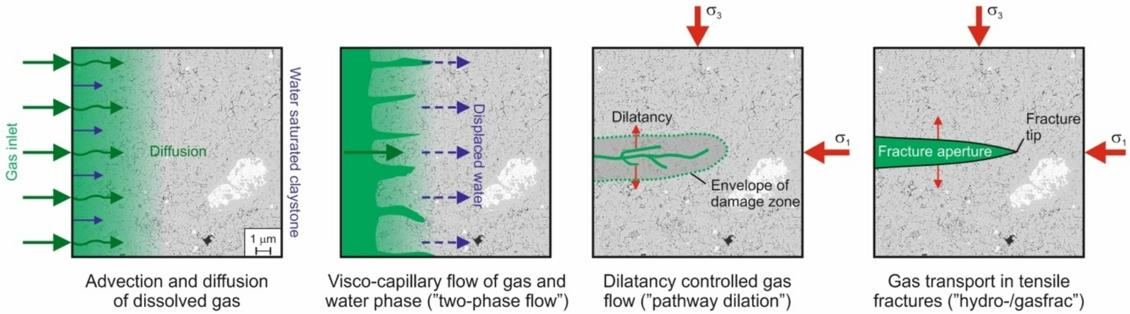

PRESENTED BY

Yifeng Wang, Teklu Hadgu, Tom Dewers, Carlos Jove-Colon, Edward Matteo (SNL), Boris Faybishenko (LBNL)

SAND2020-12777 PE

Time series analyses

Segmentation of inflow and outflow time series based on time variation of the injection pressure

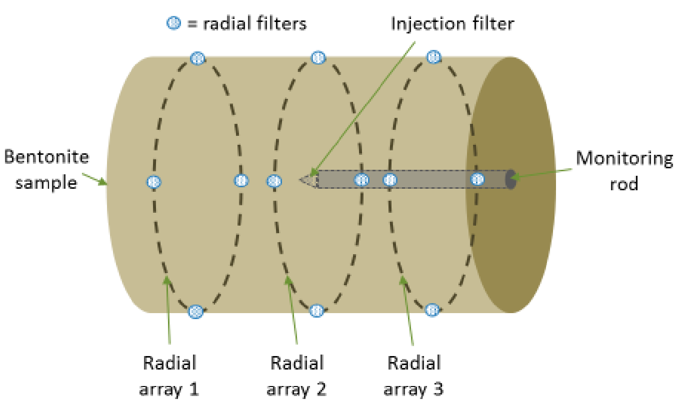

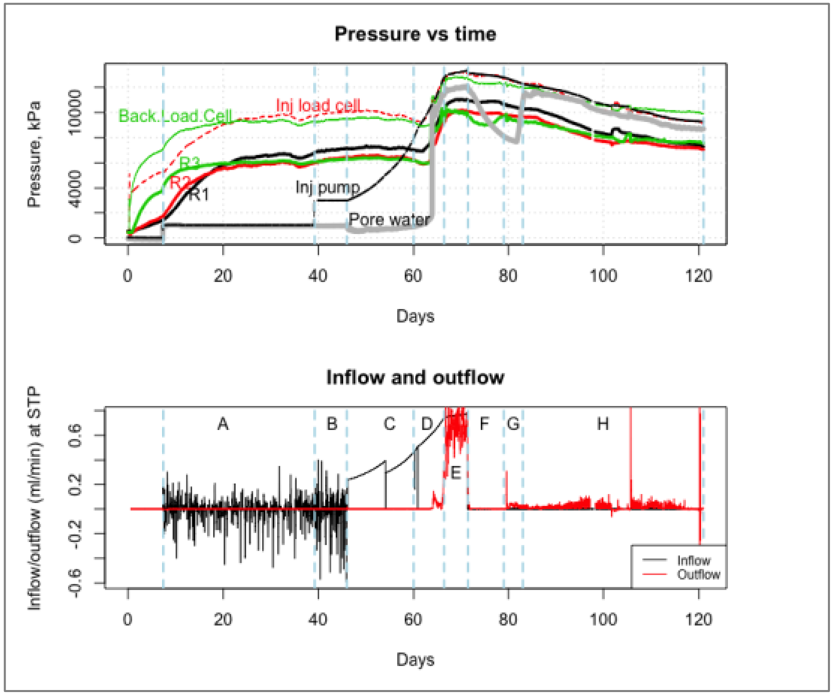

Segments A and B for the inflow, and Segments E and H for outflow were selected for further time series analysis

Global embedding dimension

Evaluation of the Global Embedding Dimension (GED=4-5) indicates phenomena of low-dimensional chaos with both deterministic and small stochastic components

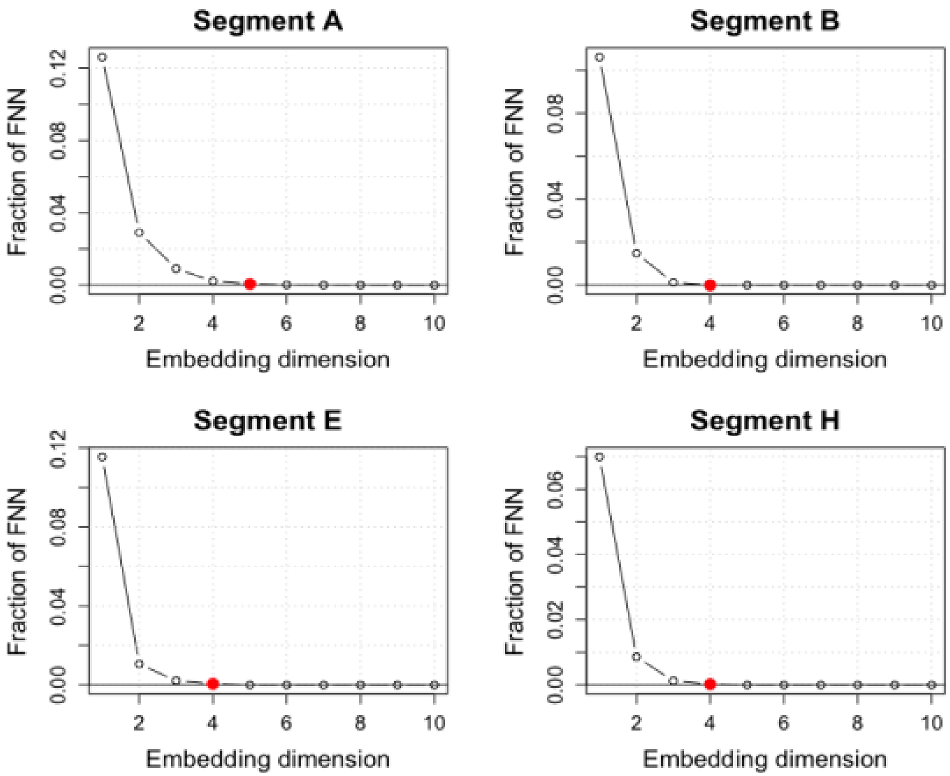

Global Embedding Dimension was calculated using the False Nearest Neighbors Method

Gas migration through channeling

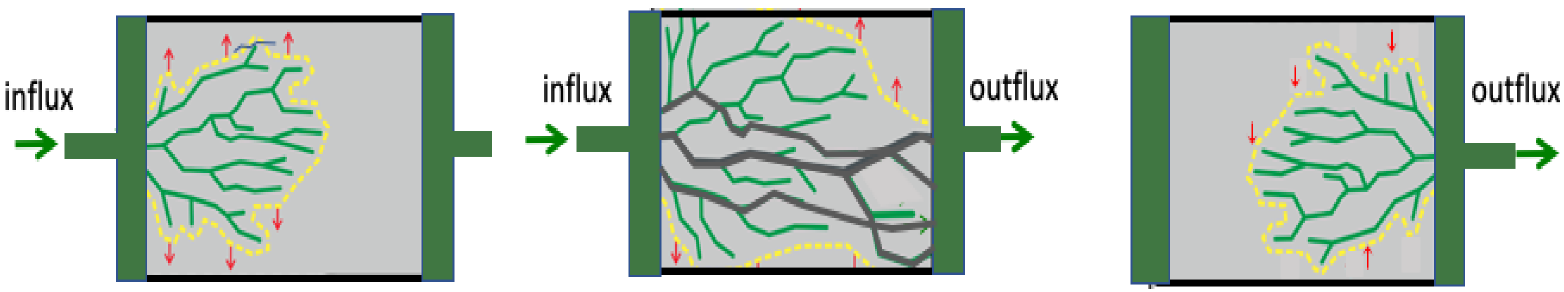

Chaotic diffusion prior to gas breakthrough

Chaotic advection post gas breakthrough

Chaotic diffusion during the bentonite recovery

Immiscible fluid invasion in deformable media

Domain I: Gas + bentonite

Domain II: Water + bentonite

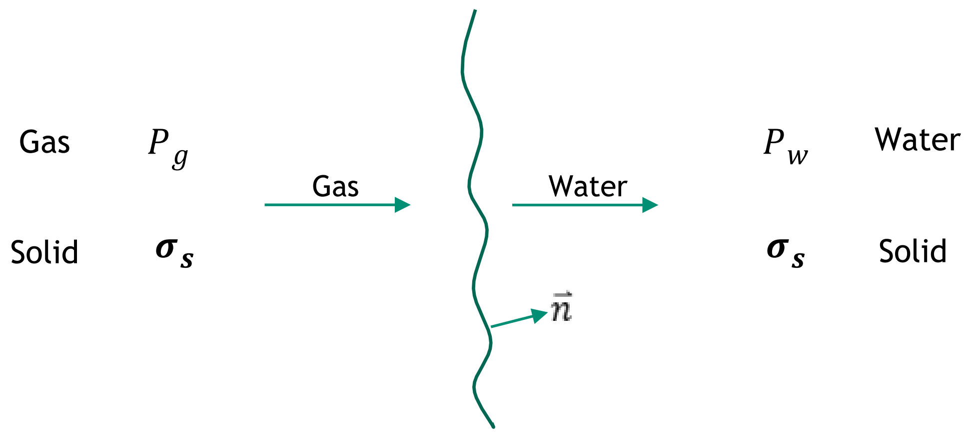

F(x, y, z, t) = 0

Domain I

Continuity for mass:

$$\frac{\partial(\phi\rho_g)}{\partial t} + \nabla\cdot(\phi\rho_g\vec{V}_g) = 0$$

$$\frac{\partial[(1-\phi)\rho_s]}{\partial t} + \nabla\cdot[(1-\phi)\rho_s\vec{V}_s] = 0$$

Continuity for momentum:

$$\vec{I} + \nabla\cdot[(1-\phi)\boldsymbol{\sigma}_s]=0$$

$$-\vec{I} + \nabla\cdot(\phi\boldsymbol{\sigma}_g)=0$$

$$\vec{I} = \frac{\mu_g}{k}(\vec{V}_g - \vec{V}_s) - P_g\nabla\cdot\phi$$

Constitutive relationship:

$$\sigma_{g_{ij}} = -P_g\delta_{ij}$$

$$\sigma_{s_{ij}} = -P_g\delta_{ij} + \zeta\delta_{ij}\frac{\partial v_{sl}}{\partial x_l} + \eta\left(\frac{\partial v_{si}}{\partial x_j} + \frac{\partial v_{sj}}{\partial x_i} - \frac{2}{3}\delta_{ij}\frac{\partial v_{sl}}{\partial x_l}\right)$$

$$P_g = \frac{RT}{\phi M_g}\rho_g$$

Domain II

Continuity for mass:

$$\frac{\partial(\phi\rho_w)}{\partial t} + \nabla\cdot(\phi\rho_w\vec{V}_w) = 0$$

$$\frac{\partial[(1-\phi)\rho_s]}{\partial t} + \nabla\cdot[(1-\phi)\rho_s\vec{V}_s] = 0$$

Continuity for momentum:

$$\vec{I} + \nabla\cdot[(1-\phi)\boldsymbol{\sigma}_s]=0$$

$$-\vec{I} + \nabla\cdot(\phi\boldsymbol{\sigma}_w)=0$$

$$\vec{I} = \frac{\mu_w}{k}(\vec{V}_w - \vec{V}_s) - P_w\nabla\cdot\phi$$

Constitutive relationship:

$$\sigma_{w_{ij}} = -P_w\delta_{ij}$$

$$\sigma_{s_{ij}} = -P_w\delta_{ij} + \zeta\delta_{ij}\frac{\partial v_{sl}}{\partial x_l} + \eta\left(\frac{\partial v_{si}}{\partial x_j} + \frac{\partial v_{sj}}{\partial x_i} - \frac{2}{3}\delta_{ij}\frac{\partial v_{sl}}{\partial x_l}\right)$$

Model formulation: At water-gas interface F(x, y, z, t)=0

$\sigma_g \cdot \vec{n} = \sigma_w \cdot \vec{n} + (\sigma^* \nabla \cdot \vec{n} + P_c)\vec{n}$ Stress balance for fluids

$[(1-\phi)\sigma_s \cdot \vec{n}]_-^+ = \phi(\sigma^* \nabla \cdot \vec{n} + P_c)\vec{n}$ Stress balance for solid

$P_c = \dfrac{2\sigma\cos(\theta)}{r}$ Capillary pressure, *r* is the pore size

$\vec{V}_w = \vec{V}_g$

$\vec{V}_w \cdot \nabla F + \frac{\partial F}{\partial t} = 0$ Kinematic evolution of displacement front

$\vec{n} = \dfrac{\nabla F}{|\nabla F|}$ Normal unit vector

Since the pore size is very small (~ nm), the capillary pressure to be overcome is very high. → The system reduces to a system of two superposed viscous fluids.

Rayleigh-Taylor instability

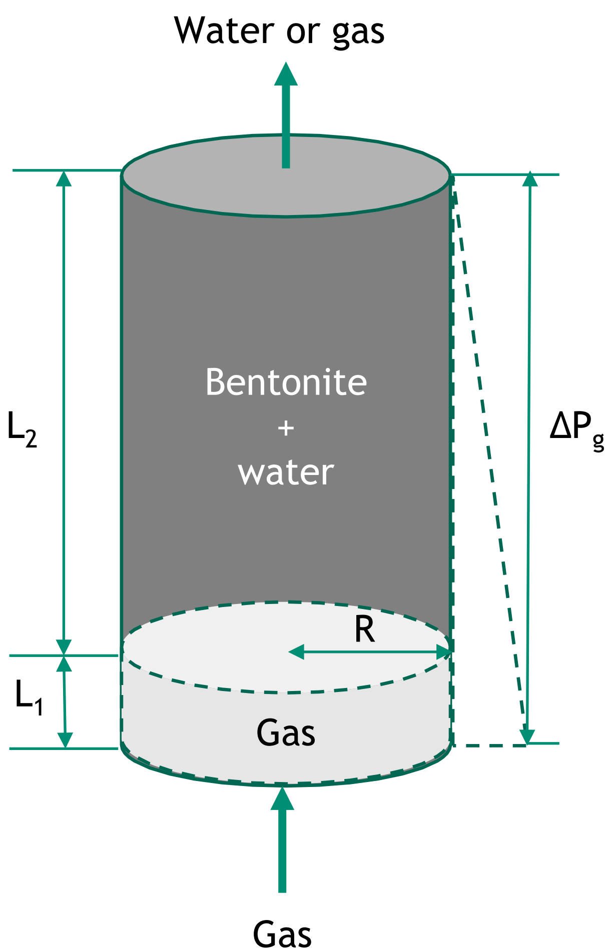

Pressurized gas tries to escape through the top vent → Rayleigh-Taylor instability.

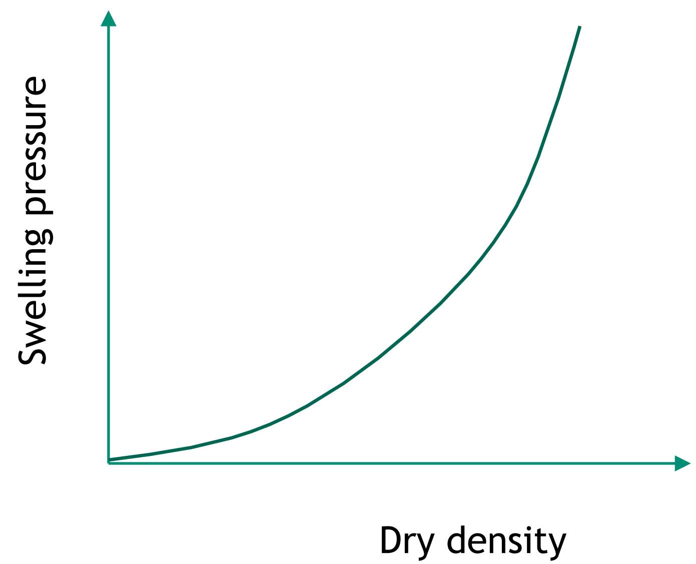

If gas migrates through channeling, the gas saturation degree would be ~$L_1/(L_1+L_2)$, which is relatively small and determined by the swelling pressure curve.

Limited gas saturation degree

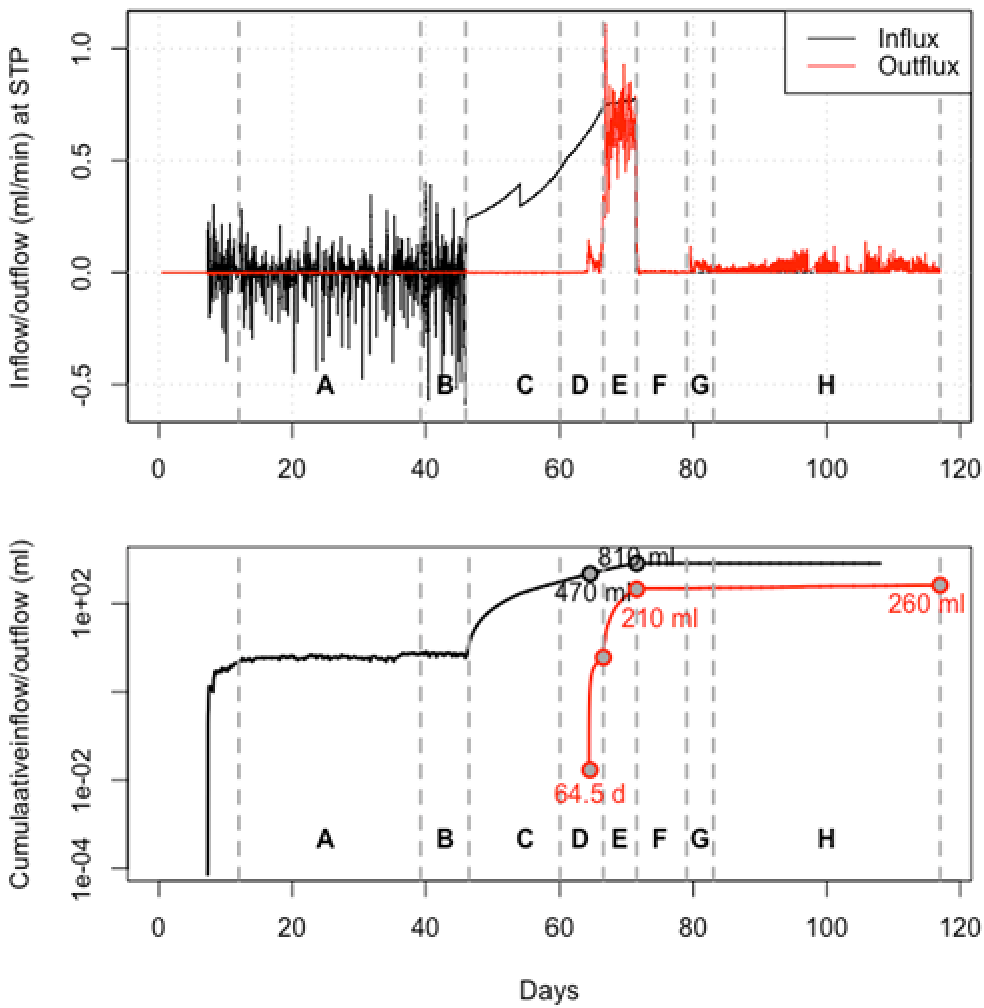

Linear instability analysis (Whitehead & Luther, 1975)

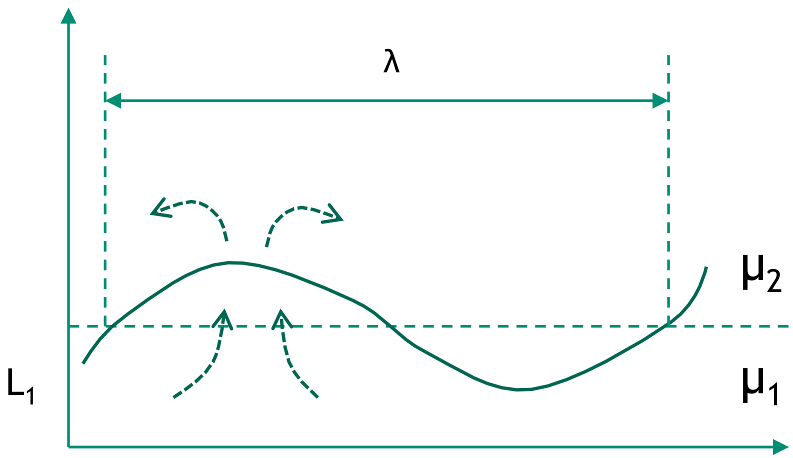

Channel separation: $$\lambda = \frac{2\pi L_1}{3^{1/3}}\left(\frac{\mu_2}{\mu_1}\right)^{1/3}$$

Growth rate of perturbation: $$\xi = \frac{2\Delta P_g L_1}{3(L_1 + L_2)\mu_2}\left(\frac{\mu_2}{24\mu_1}\right)^{1/3}$$

- The number of channels to be developed is determined by the viscosity ratio (μ_2/μ_1) only.
- The growth rate of the perturbation is determined by both the gas pressure gradient and the viscosity ratio.

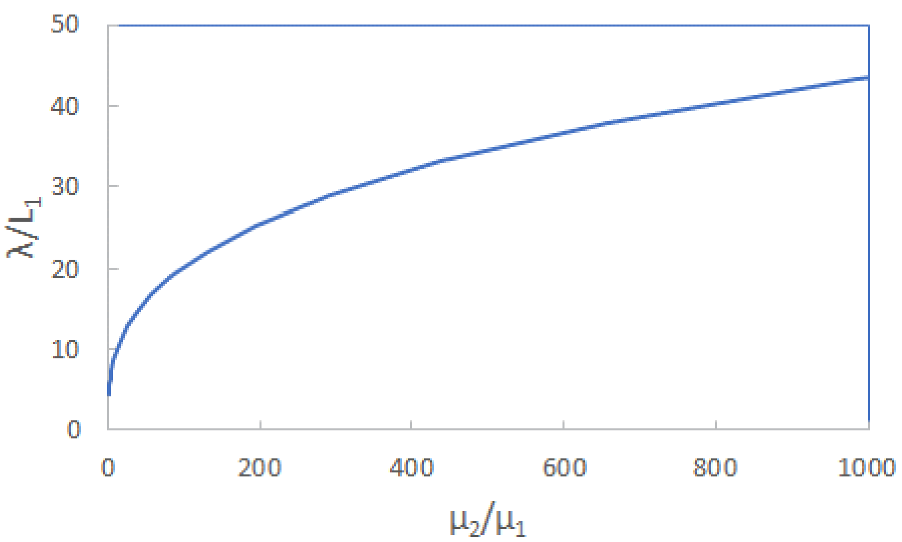

Geometry of channeling fluid (Whitehead & Luther, 1975)

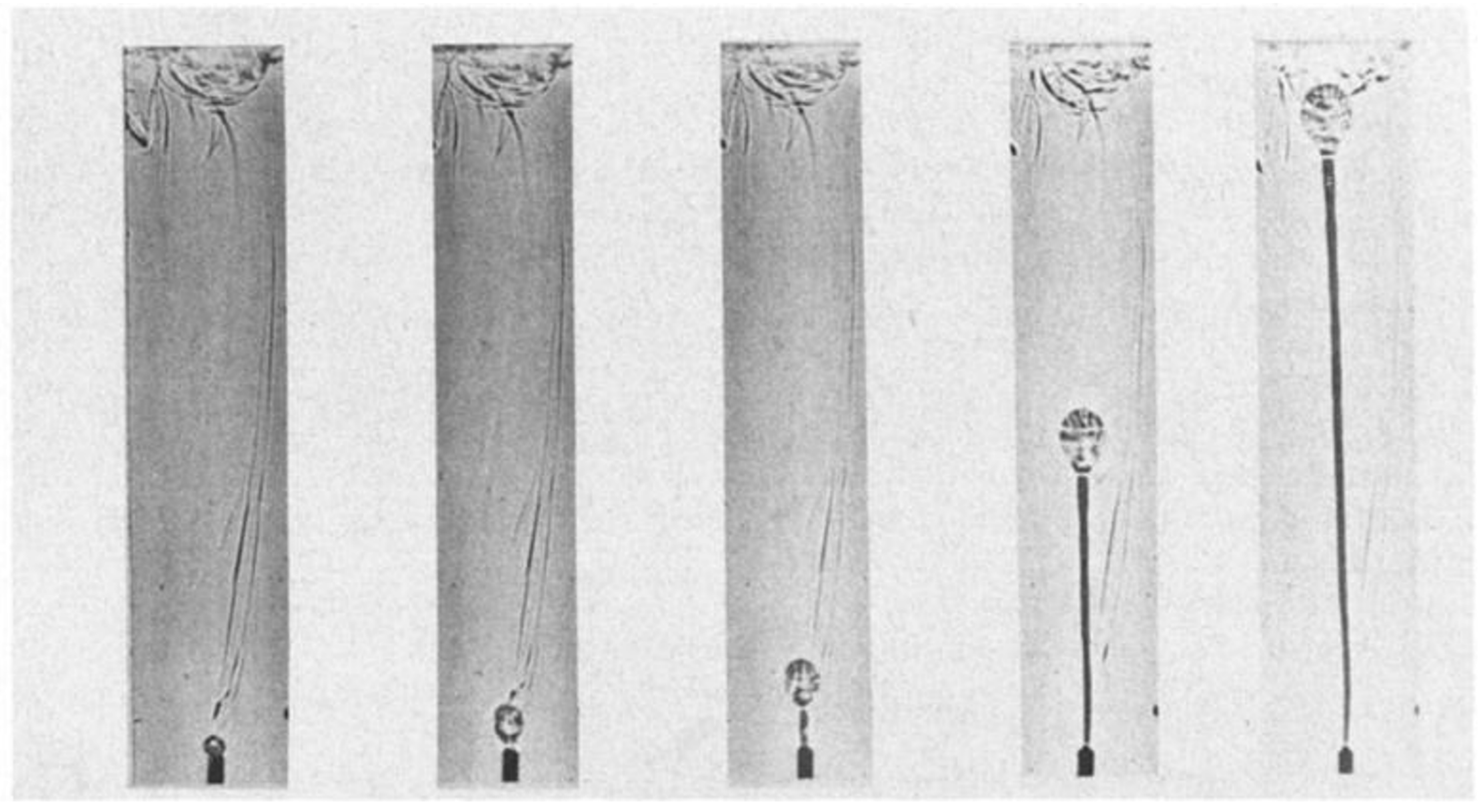

Buoyant rising of a less viscous fluid within a more viscous fluid (μ_2/μ_1 = 6000)

Gas bubble movement: Deterministic chaos

- As a gas bulb or channel nucleates and migrates in a water saturated compacted bentonite, complex nonlinear dynamics of gas flow would emerge due to the dynamic coupling between fluid flow and matrix deformation.
- The complex behaviours of the system arise from constantly unstable gas percolation fronts.

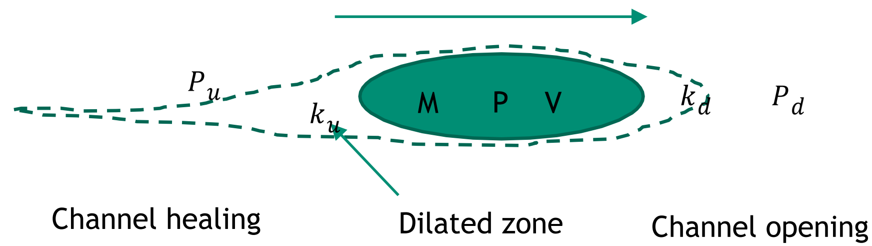

$$\frac{dP}{dt} = \lambda_1 p \left(1 - \frac{P}{K}\right)$$

$$P_{n+1} = P_n + \lambda_1 P_n \left(1 - \frac{P}{K}\right) \Delta t$$

$$\lambda = 1 + \lambda_1 \Delta t$$

$$\boxed{p_{n+1} = \lambda p_n (1 - p_n)}$$

Assume stepwise movement of a bubble to overcome the threshold for bubble opening at its advancing front.

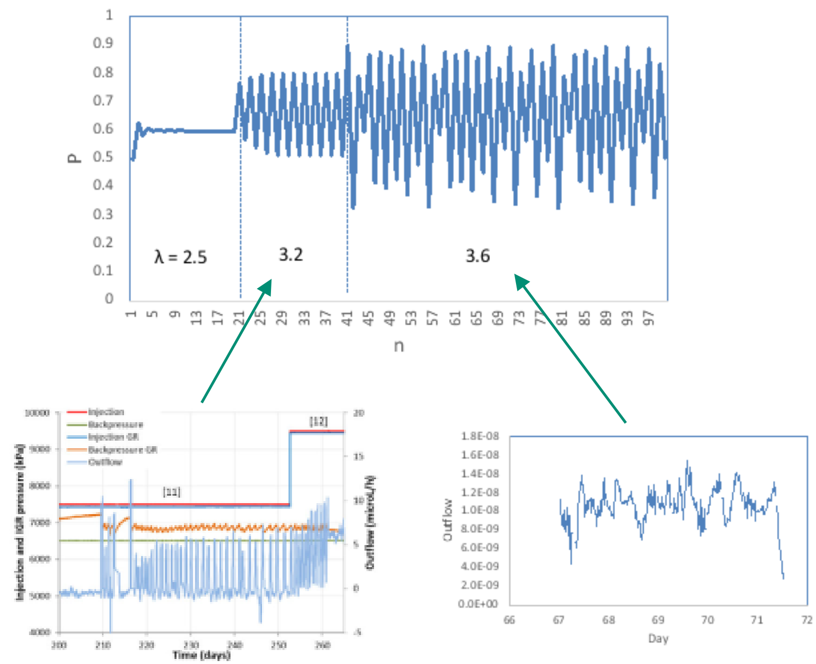

FORGE Report D4.17 (Harrington, 2013)

Instability of a single deformable gas permeation channel

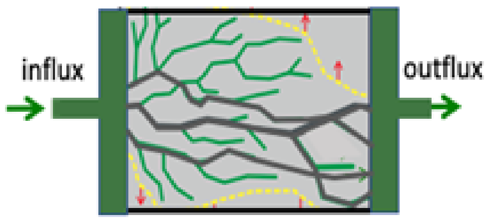

Chaotic advection post gas breakthrough

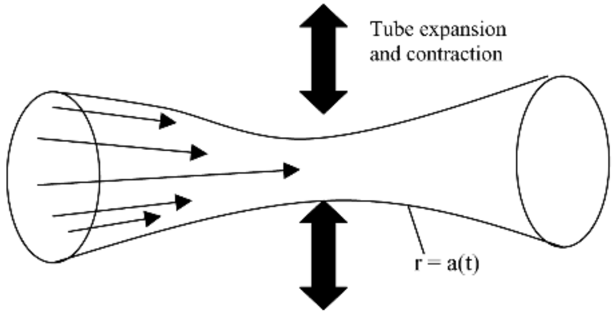

Makinde (2005)

- Model formulation
- Model analysis
- Lump parameter model
- Comparison with experimental data
    - Gas flow rate
    - Variation amplitude and frequency -> bulk material properties?

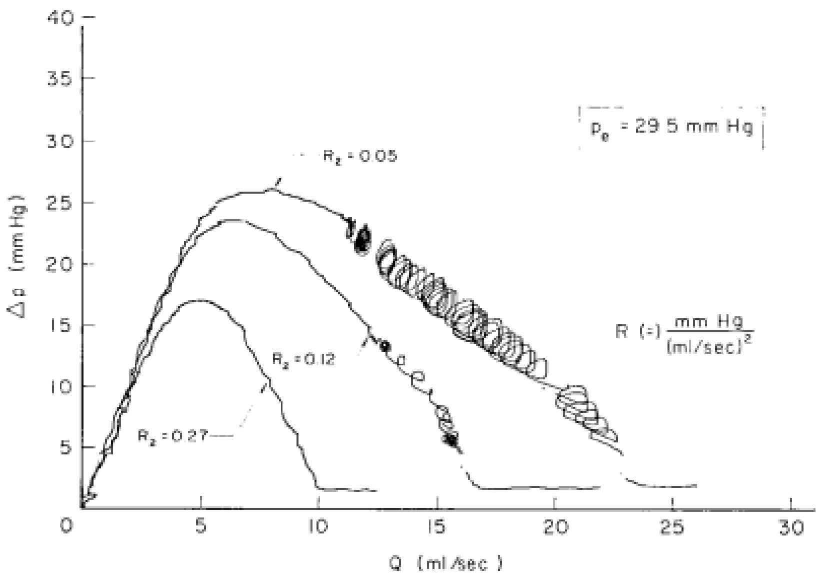

Katz et al. (1969)

Concluding remarks

- Understanding of the underlying physical process
  - Mechanistic model (3-4 variables)
- Constraints on experimental data
  - Limited gas saturation degree
  - Number of channels
  - Bubble movement
- Providing the information about relevant time and spatial scales for numerical simulations
- Providing insight about process upscaling
- Data requirements
  - High resolution sampling interval
  - Data from large-scale tests